STUDY OF WEAR PROCESSES OF WELD CLADS

Janette Brezinová[1], Anna Guzanová[1)], Pavlo Maruschak[2], Denisa Lorincová[1]*
[1] Technical University of Košice, Department of Technology and Materials, Košice, Slovakia
[2] Ternopil Ivan Pul'uj National Technical University, Department of Industrial Automation, Ternopil, Ukraine

Received 18.07.2013
Accepted 09.01.2014

**Corresponding author: Anna Guzanová, E-mail address: anna.guzanova@tuke.sk, Tel.: +421556023515, Fax: +421556225186, Technical University of Košice, Department of Technology and Materials, Mäsiarska 74, 040 01 Košice, Slovakia*

Abstract
This paper deals with the analysis of the renovation layer quality of continuous casting steel rolls, developed through the submerged arc surfacing method (SAW). The continuous casting roll was analysed via the degradation phenomena which act during the operation. Four kinds of filler materials were used for the renovation of the worn roll. Surfacing was carried out as a three-layer in order to eliminate the need for intermediate layer formation. The quality of weld deposits was evaluated in terms of the structure, hardness and wear resistance of weld deposits at 23°C and 400°C using pin-on-disc wear test. The best properties showed newly developed filler material W8-WLDC8 from the point of view of the hardness, together with wear resistance of the deposited layers in room and elevated temperatures.

Keywords: submerged arc welding, hardness, microstructure, adhesive wear, pin-on-disc

1 Introduction
Nowadays, continuous steel casting lines are widely used for casting steel. The steel casting line is the equipment for the continuous casting of steel with a slab crystallizer. The movement of the slab provides tens of rolls. Rolls are therefore one of the key elements of the line. The rolls operate under hard conditions leading to considerable wear of the rolls. The costs to change them are a very significant component of the total costs of ensuring the operation of the device.
Rolls are made of creep resistant low alloy C-Cr-Mo steel: 41CrMo4 EN 10083-1-91 or C-Cr-Mo-V: 1.7733 24CrMoV55, they are solid (forged, or cut), hollow, water-cooled inside and outside, alternately heated by a hot slab and cooled by water/steam/air cooling. The slab temperature at the beginning of the casting line is approximately 1250 °C and at the end of the line around 800 °C.
From the tribological point of view, rolls are stressed by an adhesive-abrasive and erosive wear. Movement of the hot slab on the rolls causes adhesive-abrasive wear on the surface of the rolls and the abrasive present on the roll surface (residues of casting powder, corrosive products, scales), acts as an abrasive agent and grinds/cuts the roll surface. On the surface of the roll pitting corrosion arises as a likely centre of fatigue cracks. Continuous casting rolls are water-cooled inside and outside; the cooling water is sprayed onto the surface of the roll through nozzles [1].
Spraying water containing dust and small particles induces erosive wear. This aggressive environment causes a reaction between the free hydrogen ions with the fluorine-rich slag.

DOI 10.12776/ams.v20i2.293 p-ISSN 1335-1532
e-ISSN 1338-1156

If the cooling water has a high chlorine content, their interaction in the high temperature stress causes stress corrosion, primarily in the areas of fatigue cracks. The oxidative gases (oxygen, air, water vapor, carbon dioxide, sulphur dioxide etc.) react with the metal surface and create a "layer of corrosion products" (ionic compounds). Reductive gases (hydrogen, ammonia, methane, hydrogen mixed with other gases, etc.) react with the metal or non-metallic component of the material, eventually penetrate into the metal and dissolve within them. [2] The high number of built-in rollers and need for the replacement of nearly a thousand portions of rolls every year has led to the renovation of damaged rolls, which is an economically more advantageous solution than the replacement with a new roll [3-9]. One way as to how to repair rolls is the utilization of hard surfacing technology, where the deposition of special welding layers with specific properties can extend the roll lifespan and improve their technological properties [10, 11]. The decision as to whether to repair or disable the worn roll can be made only after visual and ultrasonic checks of a turned roll surface based on the presence of defects, **Fig. 1.**

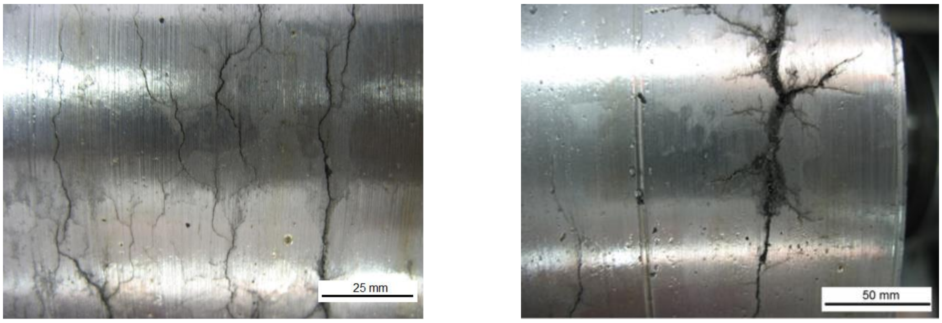

Fig. 1 Cracks on the surface of continuous steel casting roll caused by thermal fatigue

A practical criterion for disabling the roll from operation is the development of main cracks exceeding the thickness of the weld. Maximum wear acceptable for renovation is 12 mm in diameter of the functional surface of the roll and 2 mm in diameter of the pin.

2 Material and experimental methods

In the experimental part of the work, a twice-renovated roller of continuous steel casting line was treated (USS Košice, Slovakia), diameter 180 mm, made of steel X20Cr13 EN 10088-3 from the top of the curved part of the line, see **Fig. 2**. The chemical composition of the roll is shown in **Table 1**.

Table 1 Standardized chemical composition of the roll base material X20Cr13 [%]

C	Cr	Si	Mn	P	S	Fe
0,16-0,25	12,00-14,00	max 1,00	max 1,50	max 0,040	max 0,015	bal.

Mechanical properties of steel X20Cr13 [12]: tensile strength Rm = 700 ÷ 850 MPa, yield strength Rp0.2 > 500 MPa.

The steel X20Cr13 is suitable for arc welding techniques and welding in a protective atmosphere. For hard surfacing of continuous steel casting roll flux-cored wires were used.

DOI 10.12776/ams.v20i2.293 p-ISSN 1335-1532
e-ISSN 1338-1156

Chemical compositions of welding wires are in **Table 2**. For welding was used universal flux. Weld wires were manufactured by COREWIRE, Ltd.

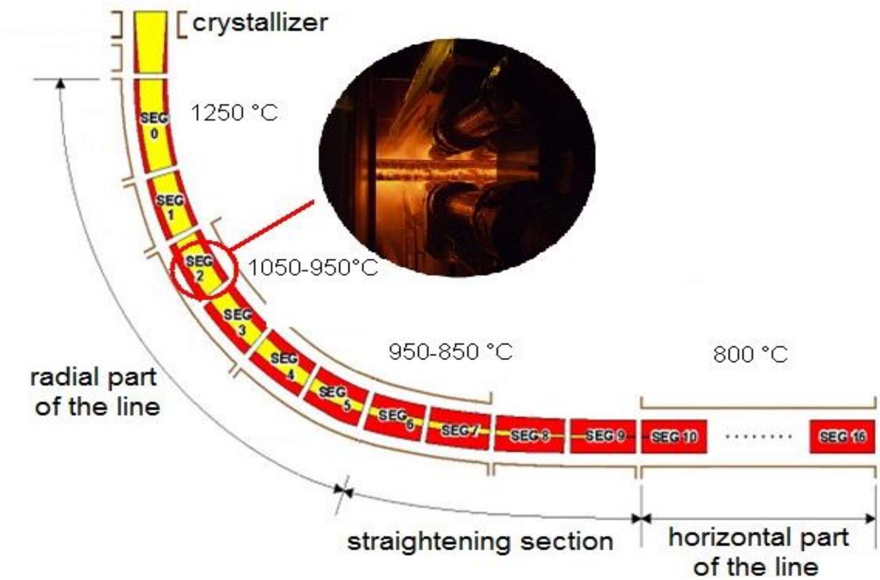

Fig. 2 Location of the roll in continuous steel casting line

Table 2 Chemical composition of welding wires used [%]

Wire	C	Si	Mn	S	P	Ni	Cr	Mo	Nb	V
WLDC 2	0.12	0.6	1.0	0.01	0.01	2.92	12.0	-	-	-
Good resistance against thermal fatigue, corrosion and wear.										
WLDC 3	0.1	0.6	1.0	-	-	2.5	12.2	0.8	0.15	0.15
Cored wire for submerged arc welding of multilayer deposits on the functional surfaces.										
WLDC 5Mod	0.25	0.6	1.0	-	-	0.25	9.0	2.0	-	-
Enhanced cored wire for submerged arc welding of multilayer deposits of hot rolling mills rolls.										
WLDC 8	0.3	0.6	1.0	-	-	-	12.2	0.75	-	0.15
Cored wire for submerged arc welding of multilayer deposition of hot rolling mill rolls.										

Wires W2-WLDC 2 and W3-WLDC 3 are commonly used for the surfacing of continuous steel casting rolls. Wires W8-WLDC 8 and W5HT-WLDC 5 have not yet been used for surfacing continuous casting rolls in practice. Surfacing parameters are given in **Table 3**.

Table 3 Surfacing parameters

wire	diameter	voltage	current	oscillation
W2-WLDC2	2,4 mm	28 V	350 A	40 mm
W3-WLDC3	3,2 mm	28 V	450 A	45 mm
W5HT-WLDC5	3,2 mm	26 V	600 A	47 mm
W8-WLDC8	3,2 mm	26 V	450 A	50 mm

DOI 10.12776/ams.v20i2.293 p-ISSN 1335-1532
e-ISSN 1338-1156

The worn turned roll was placed on roll surfacing equipment Weldclad GU125LZ, COREWIRE Ltd. after preheating in electric furnace at 350 - 400 °C. On the roll base materials were subsequently deposited three layers using automatic SAW technology (method 121 STN EN ISO 4063) without interlayer. After surfacing, the roll was cooled down in an electric furnace in isothermal cooling wrap (cooling rate 40 °C/h) to room temperature and subsequently was tempered at 500 °C/8 hours. After tempering, the roll slowly cooled in the furnace (cooling rate was 40 °C/h). When the roll reached a temperature of 150 °C, the roll was next cooled down to room temperature in the open air. After the deposition of weld layers and after turning the presence of surface defects in the weld deposits was checked using visual test and liquid penetrant test (STN EN ISO 23277). Subsequently, the internal defects were checked by an ultrasonic test (reflection method) according to STN EN ISO 11666. The test samples were cut from the roll mechanically, without heat affecting the use of the material (water jet technology). The microstructure of the weld deposits was evaluated on the metallographic sections [13]. The hardness of the weld deposits was measured according to the Vickers method (STN EN ISO 6507-1) on metallographic sections with a load of 294.2 N (HV 30), loading time 15 s. The wear resistance of the weld layers was evaluated in terms of adhesive wear (pin-on-disc, test temperature 23 °C and 400 °C, relative humidity 21 %, normal load 5 N, the track radius 2.5 mm, sliding distance 100 m, linear speed 5 cm.s-1, static partner: WC-Co ball, diameter 6 mm, surface roughness of the specimen before the wear test: 0.1 μm). The wear of the test samples was evaluated by the coefficient of friction and wear track profile using a confocal 3D microscope in accordance with ISO 20808: 2004. Next, the wear volume of the specimen V_{disk} [mm^3] and specific wear rate of the specimen W_{disc} [mm^3. N^{-1}. m^{-1}] was calculated after loads at specified temperatures [14, 15]. Erosive wear of weld clads was simulated by abrasive blasting process in a laboratory mechanical blasting equipment KP-1 by abrasive impact test on specimens with weld clads and subsequently it was evaluated on the basis of weight loss Wh. Parameters of the test: abrasive: brown corrundum, grain size 0,71mm, impact angle: 45°, 90°, grain velocity 70,98 mps, weight of abrasive used: 1,1 kg, total number of blasting cycles: 50.

3 Results and discussion

The thickness of the individual layers of the weld deposit was determined by a macroscopic analysis of the samples. The thickness of the cover layer was 2 mm, the thickness of the first weld layer ranged from 2 to 7 mm, the thickness variation of the heat affected zone for W2-WLDC 2 and W8-WLDC 8 was 7 – 10 mm and for W3-WLDC 3 and W5HT-WLDC was 7 - 13 mm. The structure of the base material is low carbon martensite. The chemical analysis proved the presence of the Mn, Cr, Si in the base material. Mn content was 0.3 %, Cr 13.8 % and Si 0.3 %.

The microstructure of the cover layer of W2-WLDC 2 is low-carbon tempered martensite, **Fig. 3a**. The cover layer contains globular inclusions arising probably from the flux used; the acicular structure partially remains. **Fig. 3b** shows the microstructure of the cover layer W3-WLDC 3, low-carbon high tempered martensite (or sorbite) with the remains of the grain boundaries.

Fig. 4a shows the martensite structure of the weld W5HT WLDC-5 with ferrite islands. **Fig. 4b** shows the structure of weld deposit W8-WLDC 8: tempered martensite with small carbide particles.

DOI 10.12776/ams.v20i2.293 p-ISSN 1335-1532
e-ISSN 1338-1156

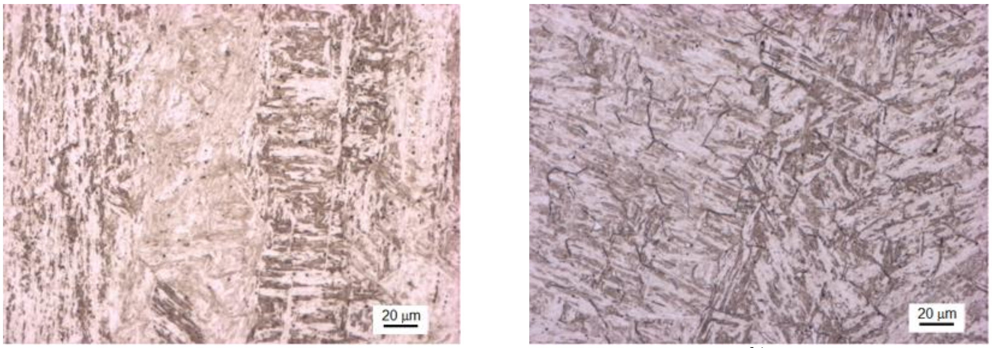

a) b)

Fig. 3 Microstructure of cover layer of weld deposits a) W2-WLDC 2, b) W3-WLDC 3

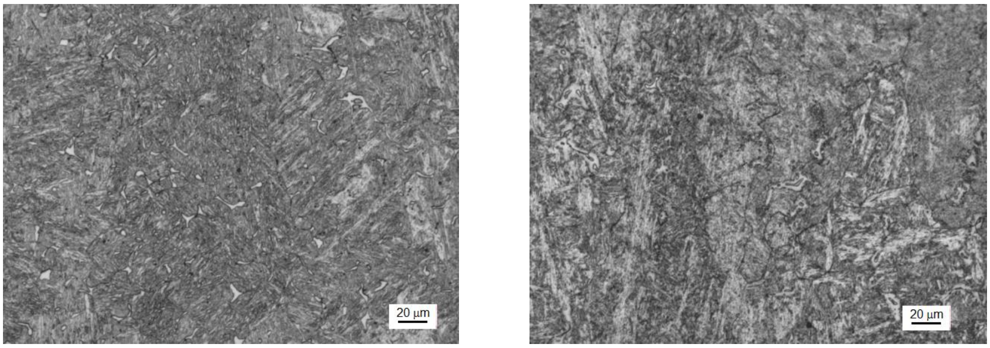

a) b)

Fig. 4 Microstructure of cover layer of weld deposits a) W5HT-WLDC 5, b) W8-WLDC 8

The hardness of the weld deposits was measured on metallographic sections from the functional surface of the roll to the base material, see **Fig. 5**.

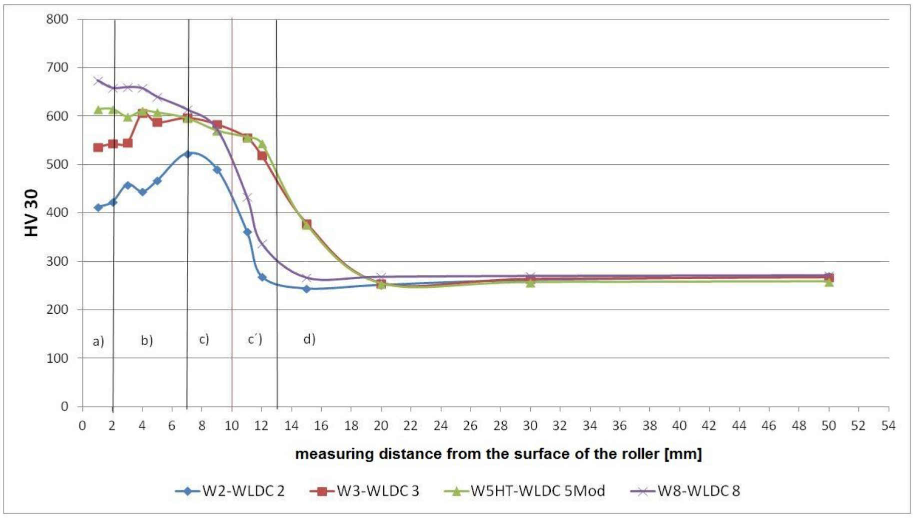

Fig. 5 Average values of surfacing layers hardness

DOI 10.12776/ams.v20i2.293
p-ISSN 1335-1532
e-ISSN 1338-1156

The highest average hardness was found in the cover layer of weld W8-WLDC 8 at a distance of 1 mm below the roll surface, where it reached a value of 675 HV 30. The lowest hardness (412 HV 30) 1 mm below the surface was weld W2- WLDC. The hardness of the first surfacing layer varied in weld deposit W3-WLDC 3, W5HT-WLDC 5Mod and W8-WLDC 8 from 546 to 661 HV 30. The lowest hardness value was weld deposit W2-WLDC 2: 459 HV 30.
During hard surfacing, heat affecting the base material occurred. It caused hardness increasing in HAZ approximately by 50 % compared to the unaffected base material. Hardness in HAZ at a distance of 7 mm from the surface was 520 to 614 HV30. **Fig. 5** shows a decrease of the hardness values from the weld surface to the base material.

3.1 Evaluation of the weld deposits quality in terms of adhesive wear

At the start of the wear, the flattening of micro-peaks and the removal of material occur at the tribological contact place. **Fig. 6** shows the appearance of the weld deposit wear track and profiles of the wear track.
Different wear track shapes were obtained with regard to the test temperature. In weld deposits W2 and W3 after the adhesive test at 23 °C in the bottom of the wear track, separating micro particles of material occurred and rolling up of material on the sides of the wear track. Due to the high temperature, the wear track was of equal width. Material loss at the temperature 400 °C is significantly higher compared with the material loss at 23 °C.
Evaluation of the weld deposits W5 and W8 showed a different wear track profile at both test temperatures, there has been registered a different wear mechanism. Due to the relative mutual movement of the static partner on the surface of the test sample at 23 °C, an adhesive micro-welds fracture occurred. Due to the higher test temperature, a wear track of equal width arose. Material loss at the test temperature 400 °C is significantly higher compared to material loss at 23 °C.
Based on the measured data for the individual measured points for evaluated weld deposits, wear volume of disc specimen (V_{disc}) and specific wear rate was then calculated (W), **Table 4**.

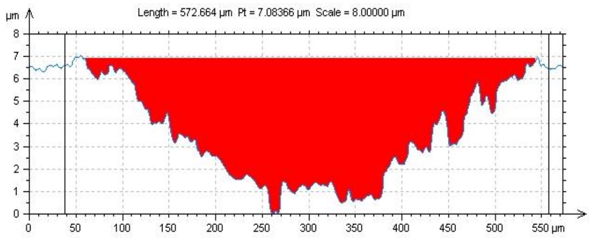

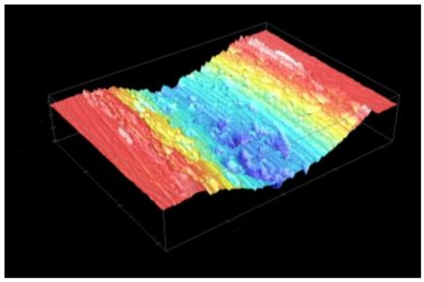

a) W2-WLDC 2, 23°C

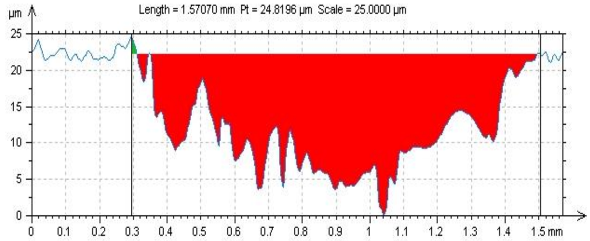

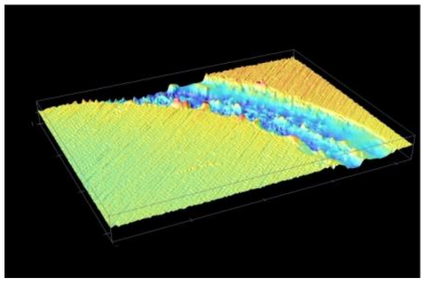

b) W2-WLDC 2, 400°C

DOI 10.12776/ams.v20i2.293 p-ISSN 1335-1532
e-ISSN 1338-1156

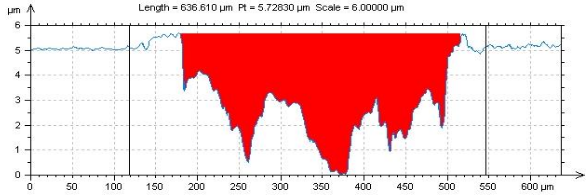

a) W3-WLDC 3, 23°C

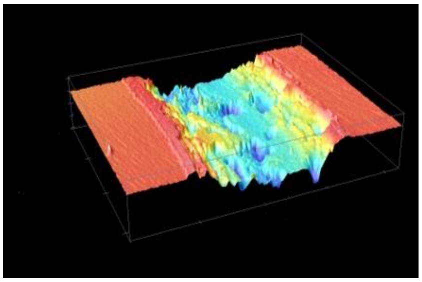

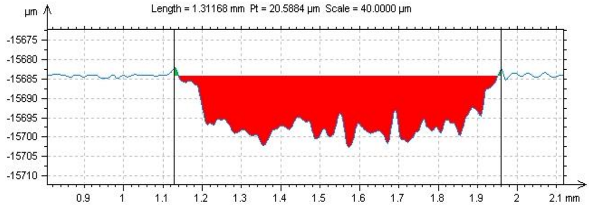

b) W3-WLDC 3, 400°C

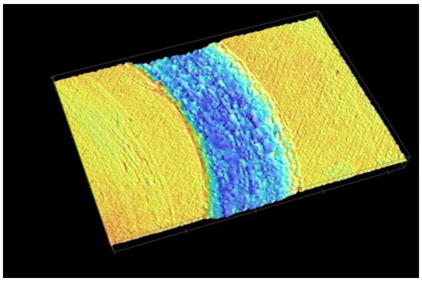

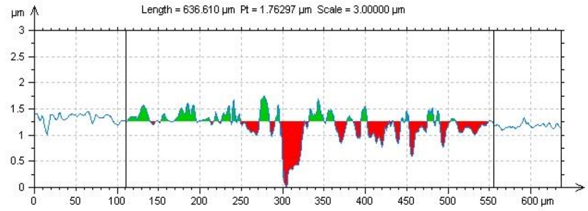

a) W5HT-WLDC 5Mod, 23°C

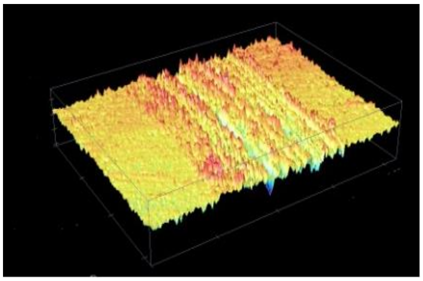

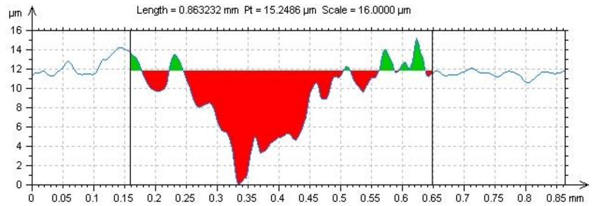

b) W5HT-WLDC 5Mod, 400°C

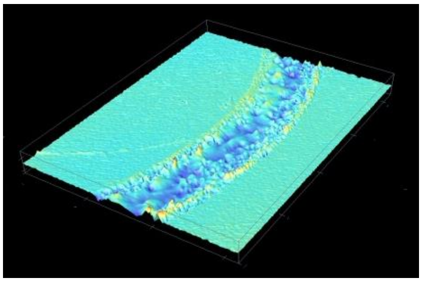

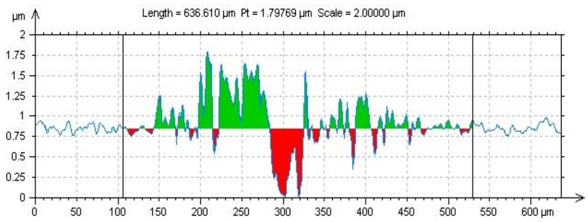

a) W8-WLDC 8, 23°C

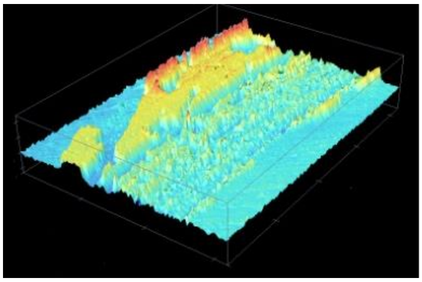

DOI 10.12776/ams.v20i2.293 p-ISSN 1335-1532
e-ISSN 1338-1156

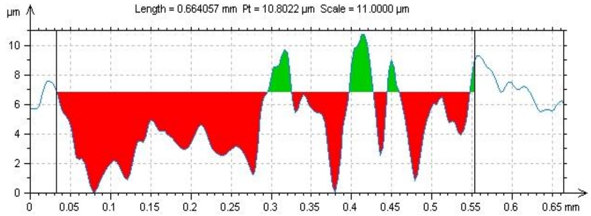

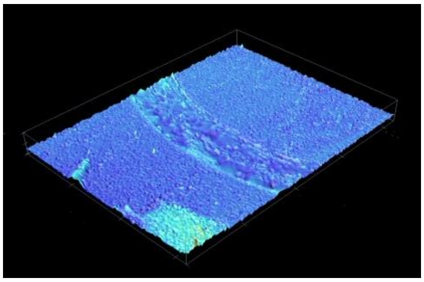

b) W8-WLDC 8, 400°C

Fig. 6 Wear track profiles and 3D view of the wear track after adhesion test at a) 23°C and b) 400°C

Table 4 Wear volume and specific wear rate of disc specimen

Weld deposit	**V_{disc} 23 °C [mm^3]**	**V_{disc} 400 °C [mm^3]**	**$W_{23\,°C}$ [$mm^3N^{-1}m^{-1}$]**	**$W_{400\,°C}$ $mm^3N^{-1}m^{-1}$]**
W2-WLDC 2	26,049	124,009	0,052	0,248
W3-WLDC 3	15,997	123,132	0,032	0,246
W5HT-WLDC 5	0,561	21,612	0,0011	0,0432
W8-WLDC 8	0,688	19,186	0,0014	0,038

At test temperature of 400 °C higher material loss occurs compared to the material loss at 23 °C. Weld deposits W2 and W3 showed a higher-order wear compared to W5 and W8. Weld deposit W8-WLDC 8 proved the highest wear resistance at the temperature of 23 °C and also at 400 °C. The lowest wear resistance was demonstrated by weld deposit W2-WLDC 2, today commercially used for the repair of the continuous steel casting rolls. The results of the wear test can be explained by the hardness, structural characteristics and chemical composition of weld wires [16,17].

The influence of the test temperature on the friction coefficient is not evident, **Fig. 7**. The highest friction coefficient was on weld deposits W2-WLDC 2 and W3-WLDC 3. Weld deposits W5HT-WLDC 5 and W8-WLDC8 showed a continuous increase of the friction coefficient depending on the sliding distance.

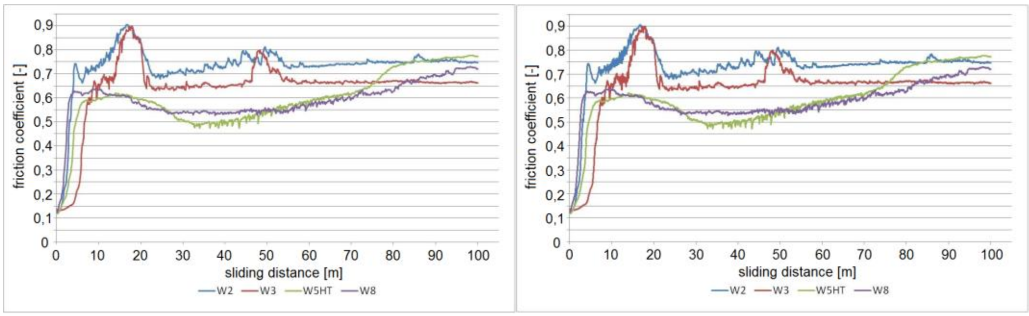

a) b)

Fig. 7 Friction coefficient of the weld deposits at the temperature a) 23°C and b) 400°C

Resistance of weld clads against erosive wear shows **Fig.8**.

DOI 10.12776/ams.v20i2.293 p-ISSN 1335-1532
e-ISSN 1338-1156

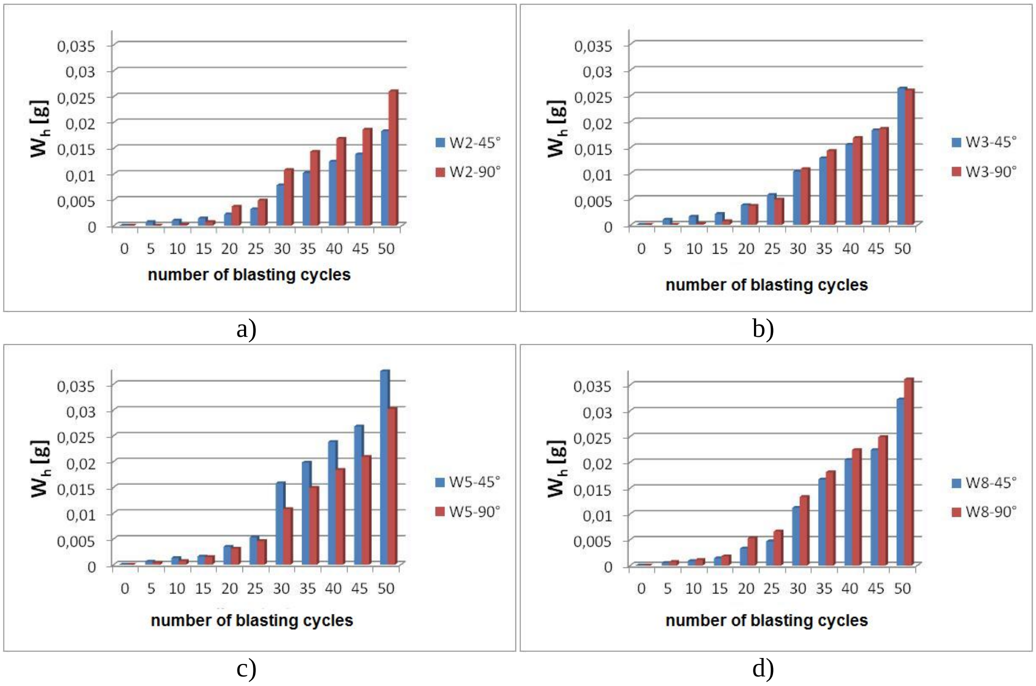

Fig. 8 Mass loss of weld clads after erosion a) W2-WLDC 2, b) W3-WLDC 3, c) W5HT-WLDC 5Mod and d) W8-WLDC 8, impact angle of abrasive 45° and 90°

Fig. 8 showed that impact angle of abrasive does affect material removal of weld clads. Weld clads W2-WLDC 2 and W8-WLDC 8 showed the greatest material removal after 50 blasting cycles at impact angle 90 °. At this angle, forging effect of abrasive grains prevails and due to depletion of weld clad plasticity fatigue failure of cladding and subsequently the release of microparticles material from the surface occured. Weld clad W5HT-WLDC 5 showed the greatest material removal at impact angle 45°, where removal of microparticles from the surface occured. It can be reasoned by the chemical composition of the cladding, mainly lower Cr content compared with other assessed weld clads [18]. Influence of abrasive impact angle on mass loss of weld clad W3-WLDC 3 has not been proved.

4 Conclusions

Based on the analysis of literature date [19,20] and the results obtained by simulation of the tribological phenomena operating in the continuous casting rolls during their operation, a newly developed welding wire WLDC W8-8 can be identified as the most suitable for the restoration of rolls of continuous steel casting line. The slightly lower wear resistance exhibited cladding made by welding wire W3-WLDC 3. This commercially used type of welding wire can also be recommended for the restoration of continuous casting rolls. Cladding made by commercially used wire W2-WLDC 2 showed the lowest tribodegradation resistance and in experimental conditions of thermal stress the weld deposit failed.

References

[1] R. Boyle, J. Frick: La Metallurgia Italiana, Vol. 2, 2005, No. 1, p. 49-52

DOI 10.12776/ams.v20i2.293
p-ISSN 1335-1532
e-ISSN 1338-1156

[2] P. Yasniy, P. Maruschak, Y. Lapusta, V. Hlado, D. Baran: Mechanics of Advanced Materials and Structures, Vol. 15, 2008, No. 6-7, p. 499-507, DOI:10.1080/15376490802142635
[3] P. Blaškovitš, M. Čomaj: *Renovácia naváraním a žiarovým striekaním* (Renovation using hard surfacing and thermal spraying), STU, Bratislava 2005 (in Slovak)
[4] M. Du Toit, B. J. Van Niekerk: *Improving the life of continuous casting rolls through submerged arc cladding with nitrogen – alloyed martensitic stainless steel*, [Available online http://www.docstoc.com/docs/47659898/improving-the-life-of-continuous-casting-rolls-through-submerged; on 20 October 2012]
[5] Z. Iždinská, A. Nasher, K. Iždinský: Materials Engineering, Vol. 17, 2010, No.1, p. 11-16
[6] J. Viňáš, J. Brezinová, A. Guzanová, P. Balog: International Journal of Materials Research, Vol. 104, 2013, No. 2, p. 183-191, DOI: 10.3139/146.110842
[7] M. Mutavdžić et al.: Materials Engineering, Vol. 19, 2012, No. 3, p. 95-103
[8] R. Paschold: Svetsaren, Vol. 56, 2001, No. 1, p. 17-19
[9] J. Brezinová, A. Guzanová, I. Mamuzić: Acta Metallurgica Slovaca, Vol. 18, 2012, No. 1, p. 20-27
[10] S. Rainwater: Submerged Arc Welding: then and now, Cleveland, Ohio 2008 [Available online http://subarcwelding.com/sub-arc-article.asp on 20 October 2012].
[11] P. Kanjilal, T. K. Pal, S. K. Majumdar: Journal of Materials Processing Technology, Vol. 171, 2006, No. 2, p. 223-231, DOI:10.1016/j.jmatprotec.2005.06.083
[12] *Stahl 1.4021 (X20Cr13)* [Avaliable online http://www.dew-stahl.com/fileadmin/files/dew-stahl.com/documents/Publikationen/Werkstoffdatenblaetter/RSH/1.4021_de.pdf; on 23 October 2012]
[13] S. Kou: Welding metallurgy, 2nd Edition. A John Wiley & Sons Inc., New Jersey 2003
[14] G. W. Stachowiak, A. W. Batchelor: *Engineering Tribology*, Third Edition, Elsevier Butterworth-Heinemann, Burlington, 2005
[15] A. Sanz: Surface and Coatings Technology, Vol. 146-147, 2001, p. 55-64
[16] T. Vuherer, P. Maruschak, I. Samardžić: Metalurgija, Vol. 51, 2012, No. 3, p. 301-304
[17] P. O. Maruschak, R. T. Bishchak, T. Vuherer: Metallurgist, Vol. 55, 2011, No. 5-6, p. 444-449
[18] V. A. Korotkov, L. V. Baskakov: Welding International, Vol. 8, 1994, No. 2, p. 129-131, DOI:10.1080/09507119409548561
[19] V. A. Korotkov, I. D. Mikhailov, D. S. Babailov: Welding International, Vol. 21, 2007, No. 7, p. 540-542, DOI:10.1080/0950711070510451
[20] V. A. Korotkov: Welding International, Vol. 12, 1998, No. 1, p. 44-46, DOI:10.1080/09507119809448965

Acknowledgement
Authors are grateful for the support of experimental works by the project VEGA No. 1/0600/13.